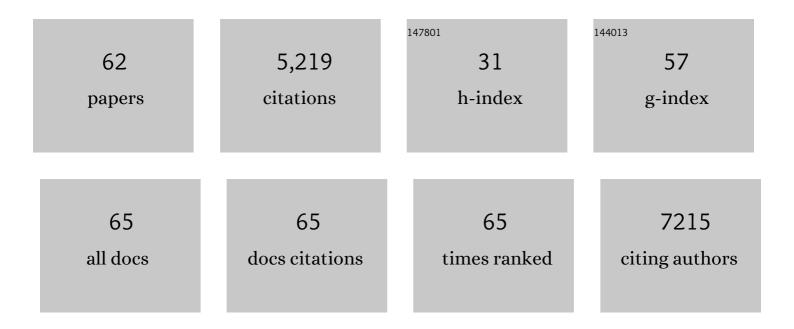
List of Publications by Year in descending order

Source: https://exaly.com/author-pdf/578531/publications.pdf Version: 2024-02-01



IULIAN MOCER

#	Article	IF	CITATIONS
1	Microplastic Ingestion by Zooplankton. Environmental Science & amp; Technology, 2013, 47, 6646-6655.	10.0	1,921
2	Uptake and Retention of Microplastics by the Shore Crab <i>Carcinus maenas</i> . Environmental Science & Technology, 2014, 48, 8823-8830.	10.0	563
3	Bioavailability of Nanoscale Metal Oxides TiO <sub>2</sub> , CeO <sub>2</sub> , and ZnO to Fish. Environmental Science & Technology, 2010, 44, 1144-1151.	10.0	251
4	Effect of Microplastic on the Gills of the Shore Crab <i>Carcinus maenas</i> . Environmental Science & Technology, 2016, 50, 5364-5369.	10.0	228
5	Sublethal toxicity of nano-titanium dioxide and carbon nanotubes in a sediment dwelling marine polychaete. Environmental Pollution, 2010, 158, 1748-1755.	7.5	177
6	Clinical applications of infrared and Raman spectroscopy: state of play and future challenges. Analyst, The, 2018, 143, 1735-1757.	3.5	163
7	Collagen fiber arrangement in normal and diseased cartilage studied by polarization sensitive nonlinear microscopy. Journal of Biomedical Optics, 2008, 13, 044020.	2.6	104
8	Effects of particle size and coating on nanoscale Ag and TiO <sub>2</sub> exposure in zebrafish ( <i>Danio rerio</i> ) embryos. Nanotoxicology, 2013, 7, 1315-1324.	3.0	98
9	Oral Particle Uptake and Organ Targeting Drives the Activity of Amphotericin B Nanoparticles. Molecular Pharmaceutics, 2015, 12, 420-431.	4.6	91
10	Imaging metal oxide nanoparticles in biological structures with CARS microscopy. Optics Express, 2008, 16, 3408.	3.4	89
11	The elastin network: its relationship with collagen and cells in articular cartilage as visualized by multiphoton microscopy. Journal of Anatomy, 2009, 215, 682-691.	1.5	80
12	Delivery of Peptides to the Blood and Brain after Oral Uptake of Quaternary Ammonium Palmitoyl Glycol Chitosan Nanoparticles. Molecular Pharmaceutics, 2012, 9, 1764-1774.	4.6	77
13	Nanofiber-Based Delivery of Therapeutic Peptides to the Brain. ACS Nano, 2013, 7, 1016-1026.	14.6	77
14	Tracing Bioavailability of ZnO Nanoparticles Using Stable Isotope Labeling. Environmental Science & Technology, 2012, 46, 12137-12145.	10.0	71
15	Evaluation of drug delivery to intact and porated skin by coherent Raman scattering and fluorescence microscopies. Journal of Controlled Release, 2014, 174, 37-42.	9.9	70
16	Label-free Chemically Specific Imaging in Planta with Stimulated Raman Scattering Microscopy. Analytical Chemistry, 2013, 85, 5055-5063.	6.5	67
17	Microstructure and antibacterial efficacy of graphene oxide nanocomposite fibres. Journal of Colloid and Interface Science, 2020, 571, 239-252.	9.4	67
18	Spectroscopy on the wing: Naturally inspired SERS substrates for biochemical analysis. Journal of Biophotonics, 2009, 2, 157-166.	2.3	62

#	Article	IF	CITATIONS
19	Exploring uptake mechanisms of oral nanomedicines using multimodal nonlinear optical microscopy. Journal of Biophotonics, 2012, 5, 458-468.	2.3	62
20	Collagen and mature elastic fibre organisation as a function of depth in the human cornea and limbus. Journal of Structural Biology, 2010, 169, 424-430.	2.8	60
21	An update: improvements in imaging perfluorocarbon-mounted plant leaves with implications for studies of plant pathology, physiology, development and cell biology. Frontiers in Plant Science, 2014, 5, 140.	3.6	53
22	Nanoparticulate peptide delivery exclusively to the brain produces tolerance free analgesia. Journal of Controlled Release, 2018, 270, 135-144.	9.9	51
23	Solute carrier family 3 member 2 (Slc3a2) controls yolk syncytial layer (YSL) formation by regulating microtubule networks in the zebrafish embryo. Proceedings of the National Academy of Sciences of the United States of America, 2012, 109, 3371-3376.	7.1	49
24	Uptake and elimination kinetics of silver nanoparticles and silver nitrate by <i>Raphidocelis subcapitata</i> : The influence of silver behaviour in solution. Nanotoxicology, 2015, 9, 686-695.	3.0	47
25	Labelâ€free imaging of polymeric nanomedicines using coherent antiâ€stokes Raman scattering microscopy. Journal of Raman Spectroscopy, 2012, 43, 681-688.	2.5	42
26	Measuring red blood cell flow dynamics in a glass capillary using Doppler optical coherence tomography and Doppler amplitude optical coherence tomography. Journal of Biomedical Optics, 2004, 9, 982.	2.6	41
27	The structure and mechanical properties of collecting lymphatic vessels: an investigation using multimodal nonlinear microscopy. Journal of Anatomy, 2010, 216, 547-555.	1.5	41
28	In Vivo Chemical and Structural Analysis of Plant Cuticular Waxes Using Stimulated Raman Scattering Microscopy. Plant Physiology, 2015, 168, 18-28.	4.8	41
29	Molecular diffusion in the human nail measured by stimulated Raman scattering microscopy. Proceedings of the National Academy of Sciences of the United States of America, 2015, 112, 7725-7730.	7.1	40
30	4-dimensional functional profiling in the convulsant-treated larval zebrafish brain. Scientific Reports, 2017, 7, 6581.	3.3	39
31	Drug delivery into microneedle-porated nails from nanoparticle reservoirs. Journal of Controlled Release, 2015, 220, 98-106.	9.9	38
32	Imaging cortical vasculature with stimulated Raman scattering and twoâ€photon photothermal lensing microscopy. Journal of Raman Spectroscopy, 2012, 43, 668-674.	2.5	33
33	Imaging the uptake of gold nanoshells in live cells using plasmon resonance enhanced four wave mixing microscopy. Optics Express, 2011, 19, 17563.	3.4	31
34	Chitosan amphiphile coating of peptide nanofibres reduces liver uptake and delivers the peptide to the brain on intravenous administration. Journal of Controlled Release, 2015, 197, 87-96.	9.9	31
35	Chemically specific imaging and inâ€situ chemical analysis of articular cartilage with stimulated Raman scattering. Journal of Biophotonics, 2013, 6, 803-814.	2.3	29
36	Lomustine Nanoparticles Enable Both Bone Marrow Sparing and High Brain Drug Levels – A Strategy for Brain Cancer Treatments. Pharmaceutical Research, 2016, 33, 1289-1303.	3.5	29

#	Article	IF	CITATIONS
37	The effect of multiple scattering on velocity profiles measured using Doppler OCT. Journal Physics D: Applied Physics, 2005, 38, 2597-2605.	2.8	26
38	Assessment of cultured fish hepatocytes for studying cellular uptake and (eco)toxicity of nanoparticles. Environmental Chemistry, 2010, 7, 36.	1.5	24
39	Tracing engineered nanomaterials in biological tissues using coherent anti-Stokes Raman scattering (CARS) microscopy – A critical review. Nanotoxicology, 2015, 9, 928-939.	3.0	21
40	lmaging microscopic distribution of antifungal agents in dandruff treatments with stimulated Raman scattering microscopy. Journal of Biomedical Optics, 2017, 22, 066003.	2.6	21
41	The Application of Fluorescence Lifetime Readouts in High-Throughput Screening. Journal of Biomolecular Screening, 2006, 11, 765-772.	2.6	20
42	Photo-induced doping and strain in exfoliated graphene. Applied Physics Letters, 2013, 103, .	3.3	18
43	Limiting the level of tertiary amines on polyamines leads to biocompatible nucleic acid vectors. International Journal of Pharmaceutics, 2017, 526, 106-124.	5.2	15
44	Ecotoxicological assessment of nanoparticle-containing acrylic copolymer dispersions in fairy shrimp and zebrafish embryos. Environmental Science: Nano, 2017, 4, 1981-1997.	4.3	15
45	A Bayesian Whittaker–Henderson smoother for generalâ€purpose and sampleâ€based spectral baseline estimation and peak extraction. Journal of Raman Spectroscopy, 2012, 43, 1299-1305.	2.5	12
46	In situ chemically specific mapping of agrochemical seed coatings using stimulated Raman scattering microscopy. Journal of Biophotonics, 2018, 11, e201800108.	2.3	7
47	Advances in nonlinear optical spectroscopies: a historical perspective of developments and applications presented at ECONOS. Journal of Raman Spectroscopy, 2016, 47, 1111-1123.	2.5	5
48	Combined effects of exposure to engineered silver nanoparticles and the water-soluble fraction of crude oil in the marine copepod Calanus finmarchicus. Aquatic Toxicology, 2020, 227, 105582.	4.0	5
49	Making microscopy count: quantitative light microscopy of dynamic processes in living plants. Journal of Microscopy, 2016, 263, 181-191.	1.8	4
50	Monitoring lipid accumulation in the green microalga <i>Botryococcus braunii</i> with frequency-modulated stimulated Raman scattering. Proceedings of SPIE, 2015, , .	0.8	2
51	Measuring blood flow dynamics using DOCT and Doppler amplitude optical coherence tomography (DAOCT). , 2003, , .		1
52	Development and applications of nonlinear optical spectroscopy: 11th ECONOS/32nd ECW meeting in Exeter (UK). Journal of Raman Spectroscopy, 2014, 45, 487-488.	2.5	1
53	Development and applications of nonlinear optical spectroscopy: 13th ECONOS/33rd ECW meeting in Dole (France). Journal of Raman Spectroscopy, 2015, 46, 677-678.	2.5	1
54	Development and applications of nonlinear optical spectroscopy: 14th ECONOS/34th ECW meeting in Leuven (Belgium). Journal of Raman Spectroscopy, 2016, 47, 1109-1110.	2.5	1

#	Article	IF	CITATIONS
55	Development and applications of nonlinear optical spectroscopy: 15th ECONOS/35th ECW meeting in Gothenburg (Sweden). Journal of Raman Spectroscopy, 2017, 48, 1019-1019.	2.5	1
56	Development and applications of nonlinear optical spectroscopy: 16th ECONOS/36th ECW meeting in Jena (Germany). Journal of Raman Spectroscopy, 2018, 49, 1094-1095.	2.5	1
57	Visualization of active ingredients uptake in seed coats with stimulated Raman scattering microscopy. Proceedings of SPIE, 2017, , .	0.8	1
58	Development of a phase-resolved Doppler optical coherence tomography system for use in cutaneous microcirculation research. , 2002, , .		0
59	Measurement of sinusoidal flow oscillations in a glass capillary tube using phase-resolved DOCT. , 2008, , .		0
60	Second-harmonic and two-photon imaging and polarimetry of articular cartilage. , 2007, , .		0
61	Monitoring agrochemical diffusion through cuticle wax with coherent Raman scattering. , 2018, , .		0
62	Ultra-low timing jitter, Ti:Al2O3 synchronization for stimulated Raman scattering and pump-probe microscopy. Journal of Biomedical Optics, 2020, 25, 1.	2.6	0